Human Molecular Genetics, 2011, Vol. 20, No. 17 **3437–3449**
doi:10.1093/hmg/ddr252
Advance Access published on June 13, 2011

Genomic, genetic and functional dissection of bitter taste responses to artificial sweeteners

Natacha Roudnitzky[1], Bernd Bufe[1,†], Sophie Thalmann[1], Christina Kuhn[1,‡], Howard C. Gunn[2], Chao Xing[2], Bill P. Crider[2], Maik Behrens[1], Wolfgang Meyerhof[1] and Stephen P. Wooding[2,*]

[1]Department of Molecular Genetics, German Institute of Human Nutrition Potsdam-Rehbruecke, Arthur-Scheunert-Allee 114-116, 14558 Nuthetal, Germany and [2]McDermott Center for Human Growth and Development, University of Texas Southwestern Medical Center, 6000 Harry Hines Boulevard, Dallas, TX 75244-8591, USA

Received March 25, 2011; Revised and Accepted June 1, 2011

Bitter taste perception is initiated by TAS2R receptors, which respond to agonists by triggering depolarization of taste bud cells. Mutations in TAS2Rs are known to affect taste phenotypes by altering receptor function. Evidence that TAS2Rs overlap in ligand specificity suggests that they may also contribute joint effects. To explore this aspect of gustation, we examined bitter perception of saccharin and acesulfame K, widely used artificial sweeteners with aversive aftertastes. Both substances are agonists of TAS2R31 and -43, which belong to a five-member subfamily (TAS2R30–46) responsive to a diverse constellation of compounds. We analyzed sequence variation and linkage structure in the ~140 kb genomic region encoding TAS2R30–46, taste responses to the two sweeteners in subjects, and functional characteristics of receptor alleles. Whole-gene sequences from *TAS2R30–46* in 60 Caucasian subjects revealed extensive diversity including 34 missense mutations, two nonsense mutations and high-frequency copy-number variants. Thirty markers, including non-synonymous variants in all five genes, were associated ($P < 0.001$) with responses to saccharin and acesulfame K. However, linkage disequilibrium (LD) in the region was high (D', $r^2 > 0.95$). Haplotype analyses revealed that most associations were spurious, arising from LD with variants in *TAS2R31*. *In vitro* assays confirmed the functional importance of four *TAS2R31* mutations, which had independent effects on receptor response. The existence of high LD spanning functionally distinct *TAS2R* loci predicts that bitter taste responses to many compounds will be strongly correlated even when they are mediated by different genes. Integrative approaches combining phenotypic, genetic and functional analysis will be essential in dissecting these complex relationships.

INTRODUCTION

Bitter taste perception is thought to act as a 'toxin detector' that warns of the presence of noxious compounds in foods, especially plant toxins such as alkaloids, which are often bitter (1). By signaling the presence of toxins, bitter taste provides protection against overexposure. In humans, this role has been reduced by technological innovations, such as cooking and agriculture. However, bitter perception continues to be an important determinant of health through its effects on behaviors, such as diet choice (2–6), alcohol consumption (7) and smoking habits (8,9). Variation in bitter taste sensitivity is substantial, and is associated with health predictors, such as vegetable intake (2), obesity (10) and possibly susceptibility to certain cancers (11). A key goal in taste psychophysics is to understand the mechanistic underpinnings of this variation.

Bitter taste responses in humans are mediated at their earliest stages by bitter taste receptors, a series of ~25 G protein-coupled receptors encoded by the *TAS2R* gene family (12–14). *TAS2R*s are expressed in taste buds, on the surface of the tongue and soft palate, where they are poised to respond to bitter compounds entering the mouth (12). When exposed to agonists, they trigger a transductional cascade that culminates in generation of a neural signal leading to perception (15).

*To whom correspondence should be addressed. Tel: +1 2146481424; Fax: +1 2146481666; Email: stephen.wooding@utsouthwestern.edu
†Present address: Department of Physiology, University of Saarland, School of Medicine, Kirrberger Straße, Building 58, 66424 Homburg/Saar, Germany.
‡Present address: National Institute of Dental and Craniofacial Research, National Institutes of Health, Bethesda, MD 20892, USA.

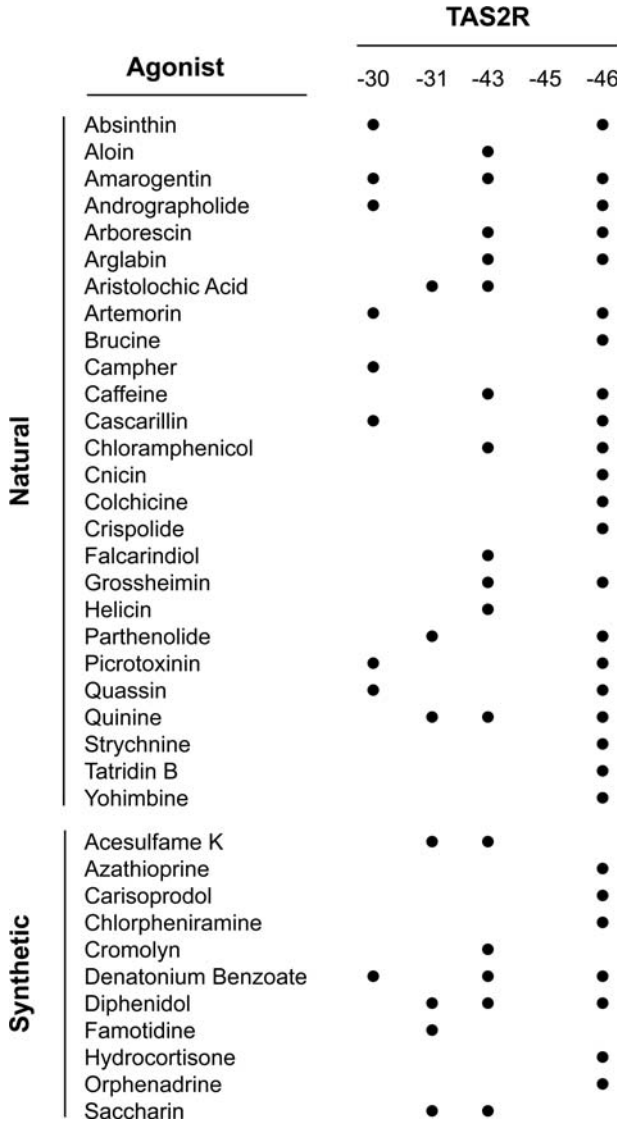

Figure 1. Known agonists of TAS2R30, -31, -43, -45 and -46. Meyerhof *et al.* (22) used cell-based functional assays to screen candidate agonists of single alleles of TAS2R30–46, revealing 26 natural and 11 synthetic compounds capable of stimulating at least one of the five receptors. Overlap in agonist specificity was extensive, with every receptor sharing at least one agonist with each other receptor. The extent to which allelic variation affects the range of agonists of each receptor is not known.

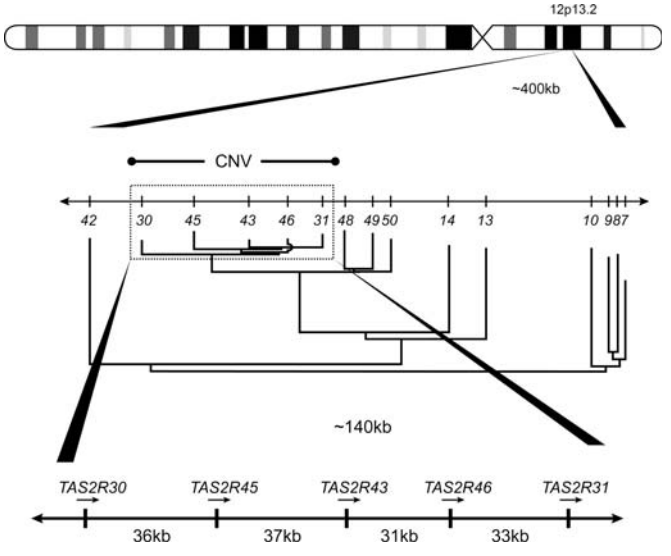

Figure 2. Genomic organization. *TAS2R30*, *-31*, *-43*, *-45* and *-46* reside in a ~140 kb region in a cluster of *TAS2R* loci spanning ~400 kb at 12p13.2, each composed of a single exon ~1 kb in length. Phylogenetic analyses by Shi *et al.* (30) revealed that *TAS2R30–46* form a tightly-related (sequence identity > 0.95) subfamily. In the J. Craig Venter genome sequence supercontig 1103279188408, they are distributed in positive (reading) orientation at intervals of 31–37 kb in non-sequential order: *TAS2R30*, *-45*, *-43*, *-46* and *-31*. Putative copy-number variants (CNVs) reported by Sudmant *et al.* (38) span the *TAS2R30–43* region.

Mounting evidence suggests that *TAS2R*s play physiological roles beyond taste perception, as well. Cells in the gut, nose and bronchi express all major components of the bitter taste transduction pathway and respond to agonists via TAS2R-mediated signaling, suggesting that TAS2Rs play generalized roles in environmental response (16–18).

Because they play a critical role in initiating transduction, mutational variation in *TAS2R*s can have profound phenotypic effects (19). For instance, alleles of *TAS2R38* account for >50% of phenotypic variance in threshold perception of phenylthiocarbamide (PTC), which ranges up to 10 000-fold among individuals (20,21). Large-scale screens have revealed that TAS2Rs as a group are capable of responding to a broad constellation of structurally diverse compounds, suggesting that individuals likely vary in ability to perceive numerous bitter substances (22). Further, TAS2Rs exhibit extensive overlap in agonist specificity (22). For instance, 15 receptors are known to respond to diphenidol (22). Thus, bitter taste responses are in many cases not a simple one-to-one function of interaction between agonists and their receptors, but a function of interactions between agonists and multiple receptors simultaneously. This, together with their potentially broad biological role, suggests that allelic diversity in *TAS2R*s could have far-reaching phenotypic consequences.

A striking characteristic of certain artificial sweeteners, including saccharin and acesulfame K, is that in addition to being perceived as intensely sweet by most individuals, they are often described as having a bitter off-taste (23–26). This property arises from agonistic interactions with TAS2R31 and TAS2R43, both of which respond to saccharin and acesulfame K at low concentrations (22,27,28). In addition, TAS2R31 and -43 harbor allelic variation that predicts both the perceived bitterness of saccharin in subjects and functional response in cell-based assays (29). TAS2R31 and -43 are encoded by two members of a *TAS2R* subfamily residing in a ~140 kb region at chromosome 12p13 that includes three additional loci: *TAS2R30*, *-45* and *-46* (Fig. 1) (30). It is not known whether any alleles of TAS2R30, -45 or -46 are responsive to saccharin or acesulfame K; however, their most common alleles exhibit sensitivity to a range of natural and synthetic agonists overlapping with those of TAS2R31 and -43, indicating that overlap with respect to saccharin and acesulfame K is likely (Fig. 2). Further, the genomic proximity of the loci encoding TAS2R30–46 suggests that phenotypic effects arising from mutations in these receptors, including previously reported effects arising from TAS2R31 and -43,

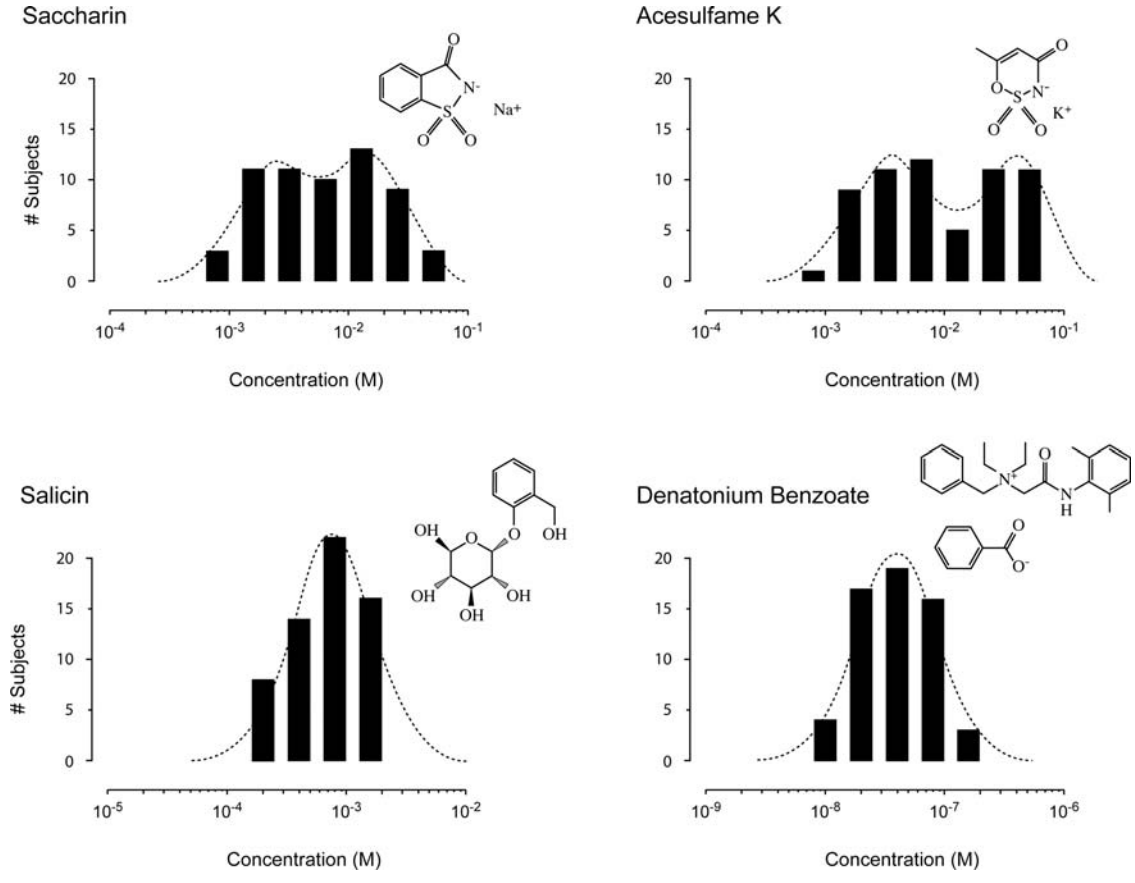

Figure 3. Threshold responses and chemical structures. Threshold responses were determined for four compounds: saccharin, acesulfame K, salicin and denatonium benzoate. Saccharin and acesulfame K are structurally similar sulfonamides used as artificial sweeteners. Salicin and denatonium benzoate, used as control substances, are structurally unrelated. For each subject, four replicate estimates were obtained and averaged. In each graph, bar height indicates the number of subjects with the given mean threshold. Threshold distributions for saccharin and acesulfame K exhibited evidence of bimodality, while those of salicin and denatonium benzoate were unimodal. Curves indicate log-normal fitted distributions.

should be correlated. To investigate the joint roles of the TAS2R30–46 subfamily in shaping perception of artificial sweeteners, we examined associations between variation in the perceived bitterness of saccharin and acesulfame K, genetic and genomic variation in *TAS2R30–46* and functional variation in receptor alleles.

RESULTS

Taste responses

Threshold perception concentrations of saccharin and acesulfame K estimated using a modified Harris–Kalmus protocol revealed extensive variation. Subjects ranged 64-fold in threshold response to both compounds, with consistent measures across replicates ($r^2 = 0.93$ and 0.92, respectively) (Fig. 3). Further, responses to the two compounds were strongly correlated ($r^2 = 0.93$). The ranges of response to saccharin and acesulfame K were substantially greater than those of two control compounds, salicin and denatonium benzoate, which varied 8–16-fold, with cross-replicate r^2 values of 0.75 and 0.86. In addition, the distributions of threshold responses to saccharin and acesulfame K were broad and slightly bimodal while those of salicin and denatonium benzoate were narrow and unimodal (Fig. 3). The threshold ranges of all three compounds differed from those reported for the well-known bitter marker compound, PTC, which elicits responses over a ~10 000-fold range and has a strongly bimodal distribution (31).

Genotypes

Whole-gene sequences obtained from *TAS2R30–46* revealed that our subjects collectively harbored 42 single-nucleotide polymorphisms (SNPs) distributed across all five genes (Fig. 4). In addition, a small in-frame (18 bp) deletion was present in *TAS2R43*. Strikingly, 86% of SNPs (36 of 42) were missense or nonsense mutations. Thirty-four encoded amino acid substitutions. Two, *TAS2R45*-A900G/X300W and *TAS2R46*-G749A/W250X, encoded premature stop codons, with the *TAS2R45* mutation predicted to truncate the encoded receptor by four amino acids and the *TAS2R46* mutation predicted to elongate the encoded protein to roughly three-quarters its normal length. This level of variation is far greater than that observed at most loci in humans (32). However, it is similar to levels reported for other *TAS2R*s, which are substantially more diverse than most human genes. For instance, the frequency of non-

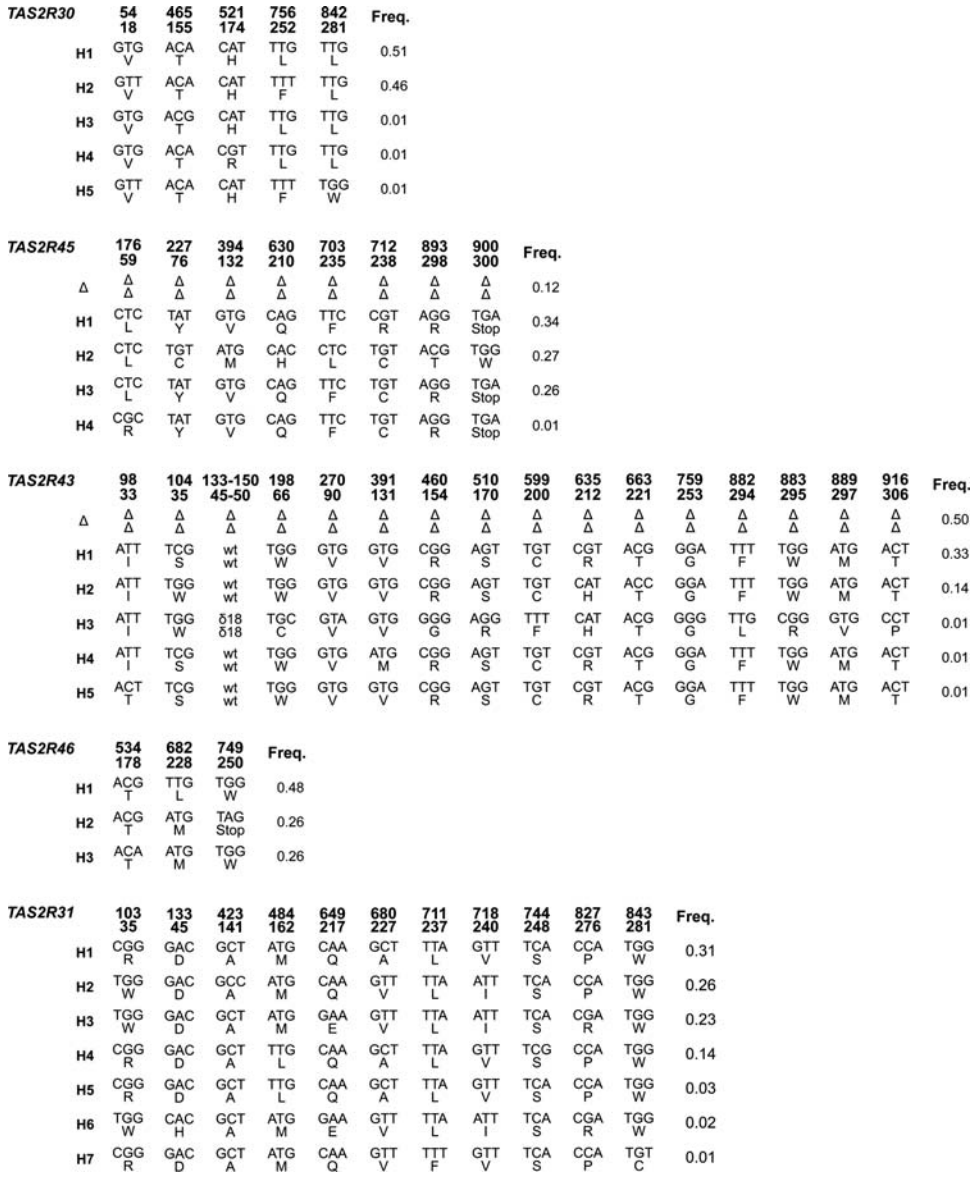

Figure 4. SNPs and haplotypes at *TAS2R30–46*. Each variable codon observed in each gene is shown, along with the alternative nucleotides and encoded amino acids. Each line represents a haplotype inferred using sequencing and/or subcloning. The frequency of each haplotype is shown in the rightmost column. Every gene examined harbored at least two haplotypes at frequencies >0.25.

synonymous SNPs in our sample, 86%, is high compared with other human genes, but is similar to the 74% observed by Kim *et al*. (33) in a survey of variation across the *TAS2R* family as a whole.

Copy-number variation

In a previous study, Pronin *et al*. (29) inferred the presence of polymorphic whole-gene deletions of *TAS2R43* and *-45* on the basis of persistent technical problems with polymerase chain reaction (PCR) amplification. However, individual genotypes with respect to the deletions, which are essential for analyzing genotype–phenotype associations, remained unresolved. Initial PCR and sequence data in our sample were consistent with the presence of the deletions identified by Pronin *et al*. (29). PCR failed to amplify *TAS2R43* in >25% of our sample, even when primers were redesigned and relocated several times (Fig. 5A). *TAS2R45* failed to amplify in a smaller number of samples. In addition, tests for Hardy–Weinberg equilibrium revealed a highly significant excess of homozygosity at both *TAS2R43* and *TAS2R45*. For instance, the C and G alleles at *TAS2R43*-C104G had allele frequencies of 0.72 and 0.28, respectively, but the genotype frequencies were 0.64, 0.16 and 0.20 for CC, CG and GG, respectively ($\chi^2 = 16.31$, d.f. = 2; $P < 0.001$) (Fig. 5D).

High rates of PCR failure and departures from Hardy–Weinberg equilibrium are both consistent with the presence of high-frequency deletion (Δ) alleles. High rates of PCR failure are explained by the fact that PCR priming sites are

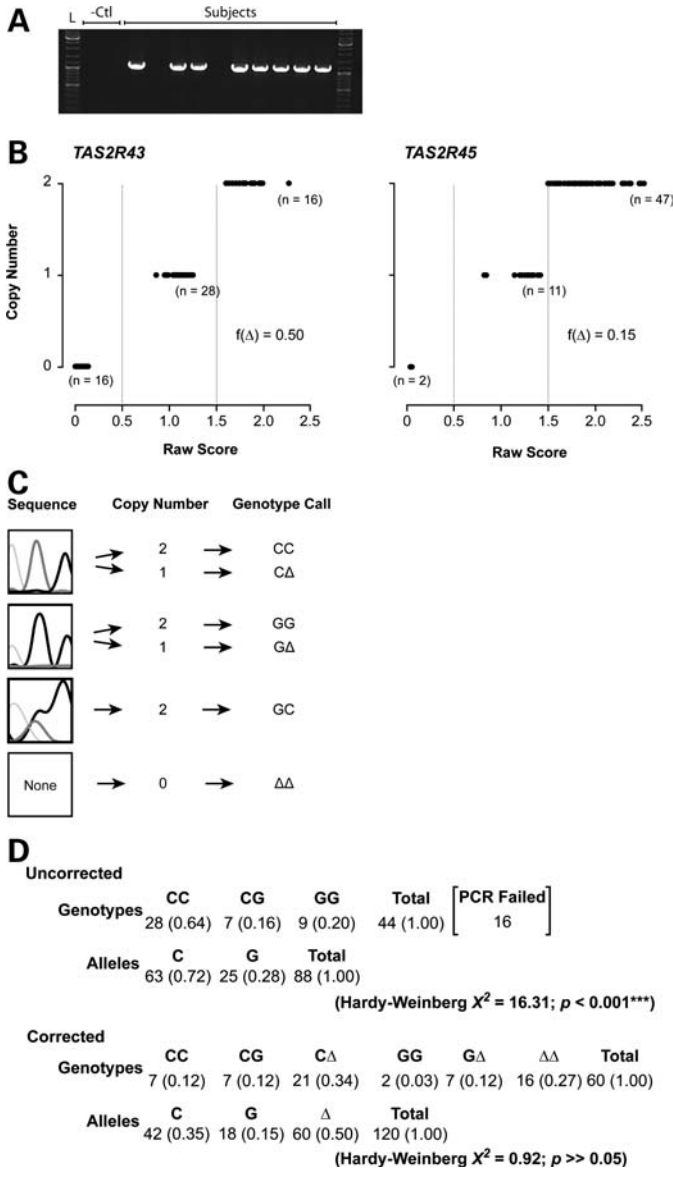

Figure 5. Copy-number variation. (**A**) In a genome-wide scan for multi-copy genes, Sudmant *et al*. (38) found evidence for major insertion/deletion polymorphisms in the *TAS2R30–46* region. Consistent with this finding, PCR failed to amplify *TAS2R43* in a large proportion of our sample, suggesting that major deletions are present. A typical gel verifying the quality of *TAS2R43* PCR product is shown. L indicates size standard; −Ctl indicates two negative PCR controls; Subjects indicates results for 10 random subjects. Empty lanes indicate PCR failures. Similar PCR failures occurred with TAS2R45. (**B**) Real-time qPCR assays distinguished individuals carrying zero, one and two copies of each gene. Raw scores in each graph represent continuous values obtained using qPCR, scaled relative to a positive control (RNAseP). Copy-number calls were determined using cutoffs at raw scores of 0.5 and 1.5 estimated copies. At *TAS2R43*, the frequency of the deleted allele (*TAS2R43*-HΔ) was 0.50. At *TAS2R45*, the frequency of the deleted allele (*TAS2R45*-HΔ) was 0.15. qPCR assays targeted at *TAS2R30*, *-31* and *-46* showed no evidence of copy-number variation. (**C**) Sequencing chromatograms alone were not sufficient to distinguish subjects homozygous with respect to a particular SNP from subjects carrying one copy of the SNP and one copy of the deleted allele. Information on copy number resolved the ambiguity by separating genotypes into those who were true homozygotes (which had a copy number of two) from those carrying one copy of the SNP allele and one deleted allele (which had a copy number of one). All SNP heterozygotes had a copy number of two. (**D**) Genotype and allele frequencies at a representative SNP (*TAS2R43*-C104G) were strongly affected by the incorporation of copy-number data into base calls. Uncorrected genotype and allele frequencies, based on DNA sequence chromatograms alone, erroneously conflated subjects homozygous for a particular SNP allele with those carrying a single copy of the allele and a deleted allele (e.g. CC could not be distinguished from CΔ). *TAS2R43* failed to amplify at all in many subjects. These effects resulted in a major excess of homozygosity, which was reflected in a highly significant ($P < 0.001$) departure from Hardy–Weinberg equilibrium. Corrected genotype and allele frequencies, determined by combining sequence and copy-number data, correctly distinguished subjects homozygous for a particular SNP allele (e.g. CC) from those carrying a single copy of the allele and a deleted allele (e.g. CΔ), as well as Δ homozygotes, bringing the sample into Hardy–Weinberg equilibrium.

completely absent from subjects homozygous for the deletion; thus, no PCR product is produced and the reactions appear to have failed. Excess homozygosity is explained because DNA sequences from subjects heterozygous with respect to the deletion come from the amplified allele only; thus, these individuals falsely appear to be homozygous at every nucleotide position. This results in departure from Hardy–Weinberg equilibrium, exactly the pattern we observed.

Copy-number assays targeting each of the five genes in our study confirmed that deletion alleles are present at both *TAS2R43* and *TAS2R45*. Assays targeting *TAS2R43* revealed 16 subjects with a copy number of zero (i.e. homozygous for the deleted allele), 28 with a copy number of one and 16 with a copy number of two (Fig. 5B). Thus, the frequency of the *TAS2R43*-Δ allele was 0.50. At *TAS2R45*, the number of subjects with copy numbers of zero, one and two were 2, 11 and 30, with the *TAS2R45*-Δ allele having a frequency of 0.15. Neither PCR dropouts nor excess homozygosity were observed at *TAS2R30*, *-31* or *-46*, and copy-number assays targeting those loci indicated that all subjects had a copy number of two, suggesting that deletion alleles are either absent or present at very low frequencies.

DNA sequence and copy-number variation were mutually consistent at both *TAS2R43* and *-45*. As expected: (i) all subjects that had previously failed to amplify by PCR were found to have copy numbers of zero (i.e. were homozygous for the deleted allele), (ii) no samples successfully amplified using PCR were found to have a copy number of zero, (iii) no samples with a copy number of one (i.e. heterozygous with respect to the deleted allele) were heterozygous at any nucleotide position, and (iv) all samples heterozygous at any nucleotide position were found to have a copy number of two (i.e. were homozygous for the non-deleted allele). Further, while genotypes based on sequence chromatogram data alone were far out of Hardy–Weinberg equilibrium, genotypes based on combined data were in near-perfect equilibrium (Fig. 5D).

Allele and genotype frequencies based on the combined copy-number and genotype data for *TAS2R43* and *-45* differed radically from estimates based sequence data alone (Fig. 5D). For instance, when the presence of *TAS2R43*-Δ was ignored, the estimated frequency of the C allele at nucleotide position 104 of the gene was 0.72. When the copy-number data were taken into account, the frequency dropped more than 50% to 0.35 (Fig. 5D). Genotype frequencies were even more strongly affected. For instance, the estimated frequency of the CC genotype was 0.64 when *TAS2R43*-Δ was not taken into account,

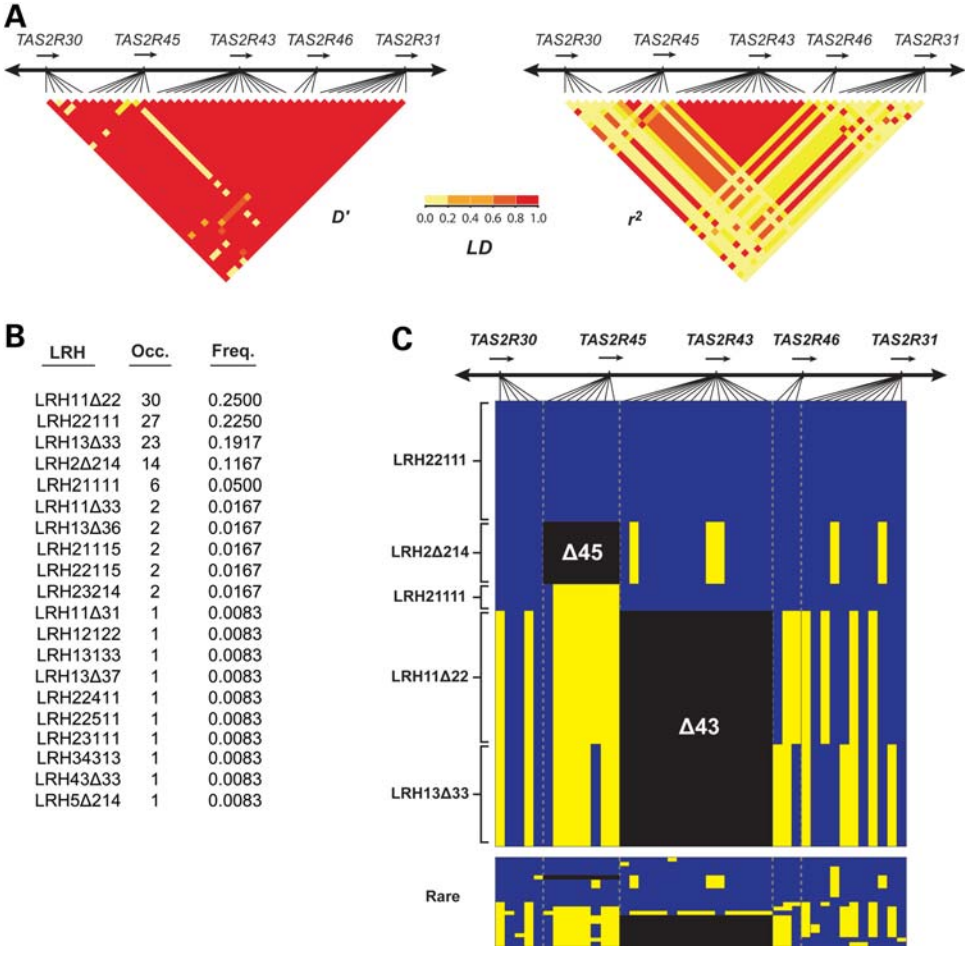

Figure 6. LD and LRHs. (**A**) LD was high across the *TAS2R30–46* region. *D′* exceeded 0.95 for nearly all SNP pairs, and r^2 exceeded 0.95 for pairs >100 kb apart. These patterns suggested that LRHs extend beyond individual genes, encompassing the entire *TAS2R30–43* region. (**B**) Inference of LRHs revealed that 20 LRHs were present, each of which could be described as a composite of the within-gene haplotypes in Figure 5. LRHs were named with respect to the within-gene haplotypes, in order of the individual genes in the genome (*TAS2R30*, *-45*, *-43*, *-46* and *-31*). For instance, LRH11Δ22 was composed of haplotype H1 of *TAS2R30*, H2 of *TAS2R31*, H Δ of *TAS2R43*, H1 of *TAS2R45*, and H2 of *TAS2R46*. (**C**) Graphically comparing LRHs and their frequencies revealed large-scale structuring in the *TAS2R30–43* region. In the graph, each column represents a SNP, with the reference allele in blue and the alternate allele in yellow. Deletion alleles of *TAS2R43* and *-45* are indicated in black. The graph illustrates the extent to which the sample was dominated by five common (frequency > 0.05) haplotypes.

and dropped more than 75%, to 0.12, when corrected. These results illustrate the critical importance of incorporating information on copy-number variation into genotype calls: failure to do so can lead to major errors in allele and genotype frequency estimates, and likely detection of genotype–phenotype associations.

Linkage disequilibrium (LD) and haplotypes

Measures of linkage disequilibrium (LD) revealed extensive correlations among sites across the *TAS2R30–46* region. *D′*, a normalized measure that provides information about the extent to which recombination has generated diversity in a region, exceeded 0.95 for nearly all pairs of sites. r^2, a raw measure of correlations among markers, exceeded 0.95 for pairs of sites >100 kb apart (Fig. 6A). High levels of LD indicate that SNPs in a region are co-segregating, which can result in spurious associations when non-functional variants are linked with truly functional variants nearby. Determination of haplotypes confirmed that genetic variation in the *TAS2R30–46* region is highly structured by LD. Within-gene analyses identified 5, 7, 6, 5 and 3 haplotypes in *TAS2R30*, *-31*, *-43*, *-45* and *-46*, respectively, including the Δ alleles at *TAS2R43* and *TAS2R45* (Fig. 4). As with individual SNPs, many haplotypes were found at high frequencies. All five loci harbored multiple haplotypes, and every locus harbored at least two haplotypes with frequencies above 25%.

Inference of long-range haplotypes (LRHs) further illustrated the extent of structuring in the *TAS2R30–46* region. Although the 42 SNPs we found could in principle recombine to form millions of LRHs, just 20 were present, and only 5 had frequencies above 0.05. Further, the within-gene haplotypes composing each LRH corresponded exactly to the within-gene haplotypes identified individually, such that each LRH could be described as a composite of five within-gene haplotypes. For example, one LRH was composed of haplotype H1 of *TAS2R30*, H2 of *TAS2R31*, H Δ of *TAS2R43*, H1 of *TAS2R45*, and H2 of *TAS2R46*. For convenience, we named

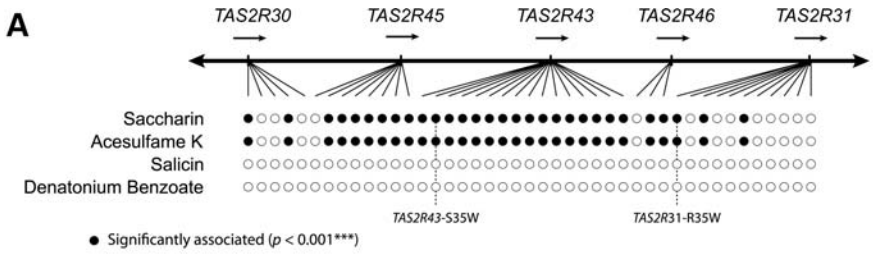

B

Gene		Log Mean Threshold (M)											
		Acesulfame K			Saccharin			Salicin			Denatonium		
		Non-Carrier	Carrier	p	Non-Carrier	Carrier	p	Non-Carrier	Carrier	p	Non-Carrier	Carrier	p
TAS2R30	H1	-1.22	-1.69	**0.004****	-1.32	-1.83	**0.004****	-2.78	-2.79	0.951	-7.09	-7.09	0.984
	H2	-1.50	-1.41	0.558	-1.64	-1.51	0.404	-2.81	-2.76	0.688	-7.14	-7.04	0.327
	Overall			**0.006****			**0.006****			0.339			0.884
TAS2R45	Δ	-1.55	-1.60	0.767	-1.66	-1.83	0.358	-2.80	-2.70	0.518	-7.06	-7.17	0.385
	H1	-1.27	-1.88	**<0.001****	-1.37	-2.12	**<0.001****	-2.76	-2.73	0.813	-7.01	-7.22	0.068
	H2	-1.61	-1.54	0.604	-1.76	-1.73	0.872	-2.74	-2.76	0.903	-7.06	-7.17	0.269
	H3	-1.55	-1.60	0.712	-1.67	-1.82	0.376	-2.74	-2.76	0.867	-7.04	-7.18	0.213
	Overall			**0.002****			**<0.001*****			0.591			0.735
TAS2R43	Δ	-1.17	-1.71	**0.003****	-1.24	-1.90	**0.001****	-2.70	-2.80	0.498	-7.04	-7.06	0.872
	H1	-1.40	-1.47	0.647	-1.54	-1.59	0.764	-2.75	-2.75	1.000	-7.06	-7.04	0.830
	H2	-1.43	-1.45	0.894	-1.49	-1.64	0.424	-2.75	-2.75	0.995	-7.07	-7.04	0.779
	Overall			**0.017***			**0.016***			0.457			0.961
TAS2R46	H1	-1.57	-1.56	0.936	-1.69	-1.69	0.979	-2.70	-2.80	0.549	-7.15	-7.03	0.383
	H2	-1.25	-1.87	**<0.001****	-1.34	-2.04	**<0.001****	-2.74	-2.77	0.812	-7.06	-7.12	0.588
	H3	-1.55	-1.58	0.857	-1.65	-1.73	0.662	-2.69	-2.82	0.353	-7.13	-7.05	0.497
	Overall			**<0.001*****			**<0.001*****			0.734			0.735
TAS2R31	H1	-1.65	-1.69	0.816	-1.83	-1.85	0.941	-2.76	-2.76	0.993	-7.05	-7.06	0.460
	H2	-1.33	-2.01	**<0.001****	-1.46	-2.22	**<0.001*****	-2.78	-2.75	0.854	-7.08	-7.13	0.617
	H3	-1.60	-1.74	0.445	-1.77	-1.91	0.467	-2.74	-2.79	0.783	-7.13	-7.09	0.762
	H4	-1.61	-1.73	0.554	-1.72	-1.96	0.275	-2.78	-2.74	0.832	-7.12	-7.09	0.798
	H5	-1.58	-1.75	0.514	-1.74	-1.94	0.508	-2.77	-2.76	0.977	-7.05	-7.16	0.583
	Overall			**<0.001*****			**<0.001*****			0.588			0.864

Figure 7. SNP and within-gene haplotype associations. (**A**) SNP-by-SNP association analyses revealed numerous sites significantly ($P < 0.001$; indicated by black circles) associated with taste responses to saccharin and acesulfame K. Significantly associated SNPs were identical for both tastants. No SNPs were significantly associated with responses to salicin or denatonium benzoate. SNPs previously reported to associate with taste response to saccharin (*TAS2R31*-R35W and *TAS2R43*-S35W) are indicated by dashed lines. (**B**) Association analyses revealed significant correlations between carrier status with respect to a single haplotype at each locus, and for each locus overall, with taste response to saccharin and acesulfame K (highlighted in grey). No haplotype at any locus was associated with response to salicin or denatonium benzoate.

LRHs in terms of their composite gene haplotypes, in order of their genomic arrangement (*TAS2R30*, *-45*, *-43*, *-46*, *-31*). For instance, the LRH described above was designated LRH11Δ22 (Figs 4 and 6B and C).

Genotype–phenotype associations

Tests for association between SNP alleles and taste responses to saccharin and acesulfame K revealed that 30 of the 42 SNP variants detected in our subjects were significantly ($P < 0.001$) correlated with both phenotypes, even after correction for multiple testing (Fig. 7A). The associations were highly similar for both compounds: all variants significantly associated with saccharin response were also significantly associated with response to acesulfame K, and all non-associated variants were non-associated for both compounds. Twenty-five of the 30 associated SNPs were non-synonymous, and every gene harbored at least one non-synonymous variant with a significant association. Twenty-three of the associated non-synonymous SNPs encoded amino acid substitutions and two (*TAS2R45*-A900G/X300W and *TAS2R46*-G749A/W250X) encoded premature stops. None of the 42 SNPs observed in our sample was associated with response to salicin or denatonium benzoate.

The most conspicuous SNP associations identified in our analyses were between *TAS2R43*-C104G/S35W, *TAS2R31*-C103T/R35W and saccharin response. This finding replicates the results of Pronin *et al*. (29), and is consistent with prior evidence that both TAS2R31 and -43 are capable of responding to both saccharin and acesulfame K (Fig. 7A) (29). In addition to replicating previously identified associations between SNPs in *TAS2R31* and *-43* and saccharin response, we identified

A

Long-Range Haplotype	Log Mean Threshold (M)											
	Acesulfame K			Saccharin			Salicin			Denatonium		
	Non-Carrier	Carrier	*p*	Non-Carrier	Carrier	*p*	Non-Carrier	Carrier	*p*	Non-Carrier	Carrier	*p*
LRH11Δ22	-1.41	-1.99	<0.001***	-1.48	-2.14	<0.001***	-2.73	-2.69	0.767	-6.98	-7.11	0.201
LRH22111	-1.74	-1.66	0.549	-1.86	-1.76	0.510	-2.73	-2.70	0.830	-7.05	-7.04	0.980
LRH13Δ33	-1.64	-1.76	0.419	-1.76	-1.86	0.511	-2.72	-2.70	0.897	-7.02	-7.07	0.693
LRH2Δ214	-1.65	-1.75	0.555	-1.74	-1.88	0.422	-2.77	-2.66	0.450	-7.03	-7.06	0.766
LRH21111	-1.57	-1.82	0.230	-1.72	-1.89	0.469	-2.74	-2.68	0.778	-7.09	-6.99	0.541
Overall			<0.001***			<0.001***			0.371			0.803

B

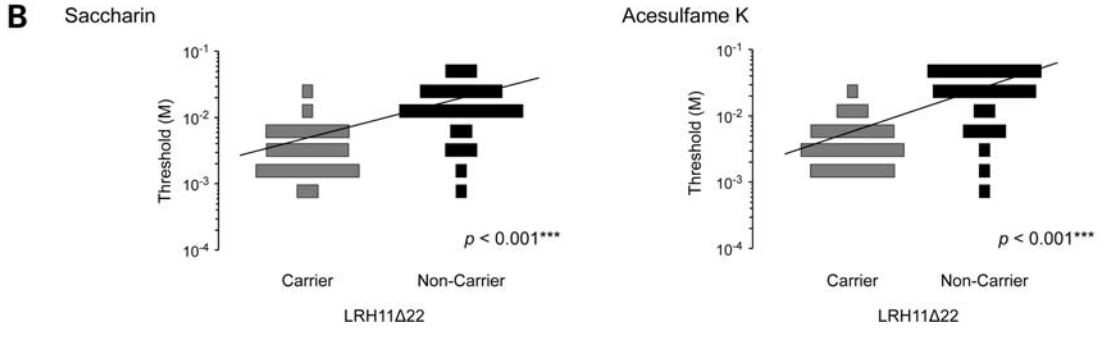

Figure 8. LRH associations. (**A**) Tests for association between LRHs and threshold responses revealed that only one haplotype, LRH11Δ22, was a significant predictor of threshold response to saccharin and acesulfame K. LRH11Δ22 was not a predictor of response to salicin or denatonium benzoate. (**B**) Violin plots illustrate the distribution of threshold responses to saccharin and acesulfame K in LRH11Δ22 carriers (i.e. homozygotes and heterozygotes) and non-carriers, which are significantly different ($P < 0.001$).

numerous associations that have not been previously reported. These included associations between non-synonymous SNPs at all five of the loci we examined, any of which could plausibly alter receptor function. This finding raised the possibility that variants in all five of the genes we examined contribute to variation in saccharin/acesulfame K response. However, this possibility was brought into question by the fact that LD was high ($D' > 0.95$) across the entire *TAS2R30–46* region (Fig. 6), which suggested that some of the associations we observed might be due to linkage between non-functional variants and functional variants.

Haplotype association tests clarified the sources of genotype–phenotype associations in our sample. Although *TAS2R30–46* each harbored multiple haplotypes, only one haplotype at each locus was significantly associated with responses to saccharin and acesulfame K: *TAS2R30*-H1, *TAS2R45*-H1, *TAS2R43*-Δ, *TAS2R46*-H2 and *TAS2R31*-H2 (Fig. 7). No haplotypes were associated with responses to salicin or denatonium benzoate. Tests for association with LRHs revealed that a single allele, LRH11Δ22, was associated with low threshold response (i.e. high sensitivity) to acesulfame K and saccharin (Fig. 8). Responses to salicin and denatonium benzoate were not associated with any LRH. Strikingly, LRH11Δ22 was composed of the five single-gene haplotypes associated with low threshold, which were in tight LD: *TAS2R30*-H1, *TAS2R45*-H1, *TAS2R43*-Δ, *TAS2R46*-H2 and *TAS2R31*-H2 (Figs 7 and 8).

The association of only LRH11Δ22 with low threshold responses reduced the number of sites that could account for phenotypic variation in our sample. LRH11Δ22 was distinguished from non-associated LRHs at just two loci: *TAS2R46* and *TAS2R31*. The other within-gene haplotypes composing LRH11Δ22, *TAS2R30*-H1, *TAS2R45*-H1 and *TAS2R43*-Δ were each present in non-associated LRHs (LRH13Δ33, LRH21111 and LRH11Δ22, respectively), and thus did not account for significant phenotypic variation. Further, the *TAS2R46* allele associated with low threshold, *TAS2R46*-H2, encodes a premature stop that truncates the receptor by ∼25%, abolishing receptor function, and is therefore unlikely to cause increased taste sensitivity. Thus, all three sites implicated in conferring low threshold occurred in *TAS2R31*: *TAS2R31*-C103T/R35W, *TAS2R31*-C649G/Q217E and *TAS2R31*-C827G/P276R.

To determine the individual contributions of *TAS2R31*-C103T/R35W, *TAS2R31*-C649G/Q217E and *TAS2R31*-C827G/P276R to the association between LRH11Δ22 and saccharin and acesulfame K thresholds, we performed analyses conditioned on genotype at each position. These analyses revealed that the *P*-value of association between LRH11Δ22 and saccharin response increased from highly significant ($P = 2.6 \times 10^{-4}$) to non-significant levels when conditioned on two of the three sites, *TAS2R31*-C649G/Q217E and *TAS2R31*-C827G/P276R, which yielded *P*-values of 0.07 and 0.11. Thus, these sites were critical to the association of LRH11Δ22 with saccharin threshold. The *P*-value of the LRH11Δ22 association also increased when conditioned on *TAS2R31*-C103T/R35W, but the increase was smaller (35-fold, from 2.6×10^{-4} to 9.3×10^{-3}) and did not render the LRH11Δ22 association non-significant. Tests for association with acesulfame K yielded similar results, with conditional

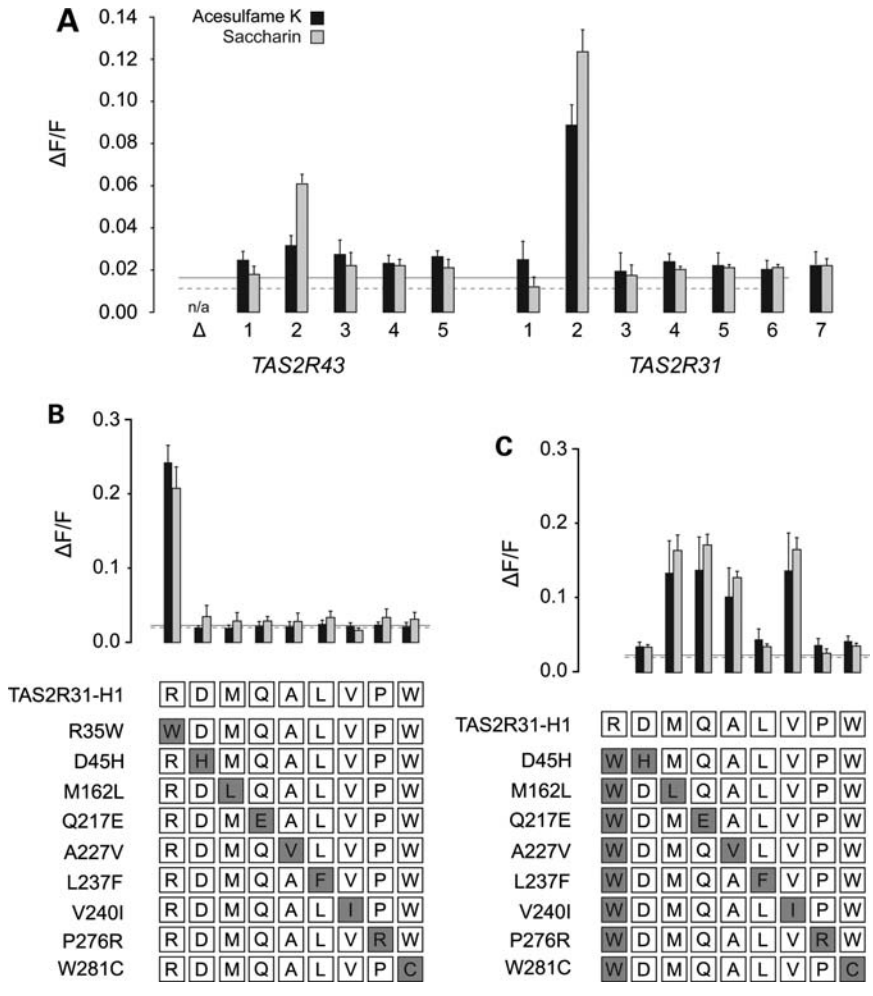

Figure 9. Functional assays. (**A**) TAS2R31-H2 was highly responsive to both saccharin and acesulfame K. TAS2R43-H2 was weakly responsive to saccharin and non-responsive to acesulfame K. (**B**) Artificial receptor constructs differing from the TAS2R31-H1 allele at each variable amino acid position in the sample (summarized in Fig. 4) revealed that only the construct introducing a W at position 35 was responsive to saccharin. In the diagram, each row represents the composition of a construct relative to TAS2R31-H1. The altered residue is highlighted in grey. Graph bars above each highlighted site indicate the functional response of the construct harboring the corresponding allele. (**C**) Artificial receptor constructs differing from TAS2R31-H1 at R35W along with a second position revealed that TAS2R31 constructs harboring W35 retained function in the presence of L162, E217, V227 and I240, but not H45, F237, R276 or C281. Results were similar for acesulfame K.

P-values increasing from 3.2×10^{-4} to 0.08, 0.07, 2.6×10^{-3} for the three sites, respectively. These findings demonstrate that the association between LRH11Δ22 and phenotypes in our sample is strongly dependent on two variants, *TAS2R31*-C649G/Q217E and *TAS2R31*-C827G/P276R, with a third site, *TAS2R31*-C103T/R35W, making a lesser contribution.

Functional variation

Cell-based assays revealed the functional underpinnings of associations between allelic variation in *TAS2R31*, *TAS2R43* and responses to saccharin and acesulfame K. Assays targeted at each TAS2R31 variant observed in our sample demonstrated that of the seven haplotypes present in our sample only one, TAS2R31-H2, was responsive to saccharin and acesulfame K. This finding supported the results of our association analyses, in which the only LRH associated with threshold responses was LRH11Δ22, which encodes TAS2R31-H2 (Fig. 9A). Assays targeted at TAS2R43, which has previously been identified as responsive to saccharin and acesulfame K (22,28), confirmed that only TAS2R43-H2 is responsive to saccharin and acesulfame K, and that the response is attenuated relative to that of TAS2R31-H2 (29,34).

To establish the functional effects of individual mutations observed in TAS2R31 in our sample, we analyzed artificial chimeric constructs of the receptor. Assays targeted at single mutant variants of the most common TAS2R31 allele, TAS2R31-H1, revealed that only constructs harboring a W at position 35 were responsive to saccharin and acesulfame K (Fig. 9B). These findings indicated that alteration of this single position was sufficient to abolish receptor function. Moreover, in the absence of W35, no other observed substitution rescued receptor function. This finding is consistent with previous reports that this mutation has important functional effects.

Double-mutant assays further established the role of mutations other than R35W in shaping TAS2R31 function. Assays targeted at chimeric variants of TAS2R31-H1 harboring both W35 and a second variant revealed that even when W35 was present, receptor function was severely attenuated or abolished by allelic variants observed at four other sites: H45, F237, R276 and C281 (Fig. 9B). Thus, these residues, like W35, are essential for receptor function. Introduction of any of them is disabling. This indicates that the genotype–phenotype relationships observed in our sample are not a simple one-to-one function of variation in TAS2R31, but a joint function of substitutions at multiple sites.

DISCUSSION

Evidence that genetic variation in *TAS2R31* and *-43* accounts for variation in the bitter perception of saccharin has suggested that variation in *TAS2R30*, *-45* and *-46*, which encode alleles responsive to many of the same agonists as TAS2R43 and -31, might affect saccharin response as well (28–30). We found that although *TAS2R30–46* harbored numerous variants associated with phenotypic responses to saccharin and acesulfame K, these associations arose principally through LD with two functional mutations in TAS2R31, *TAS2R31*-C649G/Q217E and *TAS2R31*-C827G/P276R. Further, *in vitro* analyses demonstrated that several additional variants present in TAS2R31 are capable of affecting taste response, although their frequencies are low.

A particularly important association in our sample was between variants in *TAS2R43* and responses to saccharin and acesulfame K. Previous studies have demonstrated that both TAS2R31 and -43 are capable of responding to saccharin and acesulfame K. In addition, mutational variation in both results in altered receptor response. Our functional analyses recapitulated both of these findings (Fig. 9). However, genotype–phenotype associations in our sample suggest that *TAS2R31* makes a far more important contribution to variable perception of saccharin and acesulfame K than does *TAS2R43*. While site-by-site analyses detected an association between *TAS2R43* variants and response, haplotype analyses revealed that the association was due to LD with functionally relevant sites in *TAS2R31*. Thus, while TAS2R43 is capable of responding to these compounds, and mutations in TAS2R43 affect functional response, they did not account for significant variance in perception in our sample. This may be due to the weak response of TAS2R43 to saccharin and acesulfame K relative to that of TAS2R31 (Fig. 9).

Our results also revealed an unexpected layer of complexity in the association between *TAS2R31* variants and perception of saccharin and acesulfame K. We found that while associations between *TAS2R31* and taste phenotype were driven principally by two sites, several additional polymorphisms in the gene affected receptor function. For instance, amino acid variants observed at four sites were capable of abolishing receptor response altogether. Thus, phenotypic associations arising from variability in *TAS2R31* were not simply due to the presence or absence of a single functional variant, but to the joint presence of several alleles, each of which exerts a separate effect. This finding illustrates the potentially varied avenues through which variation in *TAS2R*s can exert phenotypic effects. A potentially powerful approach for dissecting these effects would be to examine associations in African populations, which generally exhibit both lower LD and higher diversity than European populations, and hence would provide the opportunity to isolate their contributions.

An important caveat of our findings is that although our results indicate that a large fraction of variance in bitter taste responses to saccharin and acesulfame K is due to variation in *TAS2R31*, they do not rule out the possibility that genes other than *TAS2R31* contribute to bitter perception of saccharin and acesulfame K. In the case of the TAS2R30–43 subfamily, it could be that certain alleles respond to one or both compounds; however, the patterns of association in our sample indicate that they are either weak or restricted to rare variants. An additional possibility is that genes other than *TAS2R30–46* contribute to variable bitter responses to saccharin and acesulfame K. Variation in genes encoding other parts of the bitter taste transduction pathway, such as G proteins and ion channels, would seem likely to make such contributions. Recently, Fushan *et al*. (35) demonstrated that variants in *GNAT3*, which encodes α-gustducin, one of the primary components of the G protein responsible for initiating taste transduction, are associated with perception of sucrose. The participation of α-gustducin in bitter perception suggests that these variants might affect perception of saccharin and acesulfame K, as well.

Similarly, our finding that polymorphism in *TAS2R31* is the main source of variation in taste responses to saccharin and acesulfame K does not imply that *TAS2R30*, *-43*, *-45* and *-46* are not important in the perception of other compounds. Although no agonists of TAS2R45 have yet been identified, TAS2R30, -43 and -46 are each capable of responding to multiple compounds (Fig. 1). For instance, TAS2R46 responds to a variety of common molecules such as caffeine, quinine and hydrocortisone (22). Further, Reed *et al.* (36) identified highly significant associations between quinine perception and a cluster of variants centered on *TAS2R19* and overlapping *TAS2R31*. These observations, together with our finding that *TAS2R30–46* are both tightly linked and genetically diverse, suggest that individuals vary in ability to perceive numerous substances as the result of mutations at these loci, and that responses to many compounds will be strongly correlated in spite of the fact that they are mediated by different genes. Further, evidence that taste transduction pathways are active in tissues not involved in perception such as gut, nose and lung cells indicates that variation in these genes could have consequences for physiological responses other than taste.

A particularly important possibility is that copy-number variation occurs at *TAS2R* loci other than *TAS2R43* and *-45*. Because copy-number variation can result in both overrepresentation and complete absence of expressed proteins, it has the potential to have extreme effects on phenotypes. In the case of *TAS2R43* and *-45*, deletion alleles were obvious because they were present at high frequencies (0.50 and 0.15), resulting in highly abnormal PCR and genotyping results. However, because PCR failures should occur at a rate that is the square of the frequency of the deleted allele, deletions with more modest frequencies will be more difficult to detect. For instance, PCR failure rates with a deletion allele

at a frequency of 0.10 should occur at a rate of $<1\%$, with less effect on Hardy–Weinberg equilibrium, and hence could be overlooked. Thus, although no sequencing study to date has reported evidence for copy-number variation at other *TAS2R*s, such data are highly susceptible to false negatives. Directly characterizing TAS2R loci with respect to copy-number polymorphism will be essential in accurately dissecting genotype–phenotype associations underlying bitter taste responses.

MATERIALS AND METHODS

Subjects

Sixty unrelated Caucasian subjects (41 women, 19 men; age range 20–62 years, mean age 32.3 years, SD = 11.4) were recruited at the German Institute for Human Nutrition (Deutsche Institut für Ernährungsforschung) for phenotyping and genetic analysis. Subjects were pre-screened to avoid inclusion of individuals with overt taste pathologies or other obvious health problems. Each subject participated in the entire course of the study, which required genotyping and eight psychophysical phenotyping sessions.

Tastants

We determined subjects' taste responses to four compounds: acesulfame K, saccharin, salicin and denatonium benzoate (04054, 240931, S0625 and D5765; Sigma-Aldrich, Inc., St Louis, MO, USA). Saccharin has previously been demonstrated to be an agonist of receptors encoded by some alleles of *TAS2R31* and *-43* (22,28,29). Acesulfame K, like saccharin, is a sulfonamide used as an artificial sweetener and has a bitter aftertaste to some individuals (23). Acesulfame K is a known agonist of a receptor encoded by at least one allele of *TAS2R31* and *-43*, although it is not known whether taste responses to acesulfame K vary as the result of mutations at these loci (22,28). Salicin, a β-glucopyranoside, is structurally unrelated to saccharin and acesulfame K. It is a known agonist of TAS2R16, which is encoded by a locus at chromosome 7q31.1–7q31.3, and no other receptor (14,22,37). Denatonium benzoate is an agonist for numerous TAS2Rs, but not TAS2R31 or -43 (22). Thus, salicin and denatonium benzoate provided a basis for comparison and control in our study.

Taste phenotypes

Recognition thresholds were determined for each compound using a modified Harris–Kalmus protocol. In each test, subjects were challenged to identify the bitter aftertaste of a single compound, which was presented in an ascending (doubling) concentration series composed of 10 steps ranging from 1.0×10^{-4} to 5.1×10^{-2} M for saccharin and acesulfame K, eight steps from 2.5×10^{-5} to 3.2×10^{-3} M for salicin and eight steps from 1.3×10^{-5} to 1.6×10^{-7} M for denatonium benzoate. At each step, the subject reported the perceived taste of the solution and spat it out into a supplied container. When a subject proceeding through a series identified a solution as having a bitter taste, the subject was then challenged to sort a set of six cups: three cups containing 20 ml solution at the concentration described as bitter and three cups containing 20 ml solution at the preceding (one step lower) concentration. If the subject successfully sorted the set into two correct groups, that concentration was scored as the recognition threshold. If the subject failed to sort the solutions correctly, the task was repeated at the next (one step higher) concentration. Subjects were then allowed to rinse with water. Each subject evaluated one sweetener and one control substance per session. Four replicates per compound were performed over eight sessions. The sequence in which compounds were tasted was counterbalanced across subjects to avoid presentation-order and carry-over effects. Threshold distributions and cross-compound correlations were calculated based on the mean estimate for each compound within subjects, and log-normal regression analyses were performed with SigmaPlot (Systat Software, Inc., Chicago, IL, USA).

DNA sequencing

Genetic samples were obtained by extracting whole genomic DNA from saliva using PeqLab Blood DNA Kit II (PeqLab Biotechnologie GmbH, Erlangen, Germany). Open reading frames of *TAS2R30*, *-31*, *-43*, *-45* and *-46* were each sequenced in their entirety (~1 kb) in all subjects. Some evidence has suggested that an unrelated gene, *TAS2R8*, may play a peripheral role in taste responses to saccharin (29). Therefore, this gene was sequenced as well. Primers were designed with the Primer Basic Local Alignment Search Tool (Primer-BLAST) by aligning coding and flanking regions from the human genome reference sequence, and were localized ~100 bp upstream or downstream of each gene. PCR was then performed using Advantage 2 Polymerase (Clontech Laboratories Inc., Mountain View, CA, USA) to amplify the full length coding sequence. Size and quality of PCR products were tested with gel electrophoresis. After purification with High Pure PCR Product Purification Kit (F. Hoffmann-La Roche Ltd, Basel, Switzerland), products were sequenced on both strands to obtain sequence of the full coding region.

Copy-number determination

In a genome-wide survey of copy-number variation in the human genome, Sudmant *et al*. (38) demonstrated the presence of major deletions in the *TAS2R30–46* region, although the exact extent of the deletions was not established. Pronin *et al*. (29) reported high rates of PCR failure when trying to amplify *TAS2R43* and *TAS2R45*, suggesting that both of these genes are affected, and that the frequency of deletion alleles might be high. To characterize *TAS2R30–46* with respect to putative copy-number variants, we used ABI TaqMan Gene Copy Number Assays. These assays used real-time amplification of fluorescently labeled probes to determine the ratio of the quantity of a target product (here, *TAS2R30–46*) to the quantity of a stable control product (*RNaseP*). To ensure that sequences obtained from each gene represented a single locus, and not a composite of more than one, we targeted probes at regions constant across sequence reads for each gene in subjects but otherwise unique in the genome. This guaranteed that probes would detect all gene copies represented by the reads for each gene without spuriously

reporting other loci. Assay results revealed whether a given sample contains zero copy of a particular gene (i.e. is homozygous for the deletion), one copy (heterozygous for the deletion) or two copies (does not carry the deletion). We designed assays targeting each gene in our study (*TAS2R30–46*), which we used to determine copy number in all subjects.

Genotype calling

Genotypes were called by combining raw DNA sequencing results and copy-number data. Genotypes at *TAS2R30*, *-31* and *-46*, which showed no evidence of copy-number variation, were called based on sequencing data alone. Genotypes at *TAS2R43* and *-45* could not be called on the basis of raw sequencing data due to ambiguity caused by the presence of deletion (Δ) alleles. Because Δ alleles fail to amplify in PCR and sequencing reactions, individuals heterozygous for Δ alleles will appear to be homozygous with respect to all SNP positions. For example, in the case of a subject appearing to be homozygous with respect to a particular SNP (e.g. CC), it could not be determined whether the genotype was truly CC or was actually CΔ, because they appear identical on sequencing chromatograms. Information on copy number resolved this problem by enabling us to distinguish true homozygotes for a particular SNP allele (which had a copy number of two) from those carrying one copy of the SNP allele and one deleted allele (which had a copy number of one) as well as homozygotes for the Δ allele (which had a copy number of zero). Thus, genotypes in *TAS2R43* and *-45* were called with respect to three alleles (two SNP alleles and a deletion allele).

Haplotype estimation

DNA sequence data enabled us to identify most haplotypes unambiguously in subjects with zero or one variable nucleotide positions, which indicated the presence of one or two haplotypes, respectively. Subcloning from additional samples identified the remaining haplotypes. LRHs, spanning the entire ∼140 kb *TAS2R30–46* region, were inferred by analyzing variation in all five genes simultaneously using the PHASE computer program, which examines genotypes to determine the most likely configuration of alleles along a chromosome and their allocation among individuals (39).

Linkage disequilibrium

LD among markers was determined using two measures, D' and r^2 (40). These measures were used to test for correlations among each pair of SNPs identified in genotyping. In the case of *TAS2R43* and *TAS2R45*, all SNPs were triallelic, with two nucleotide alleles and a deletion allele. Therefore, these SNPs were recoded as diallelic markers by collapsing the two more weakly associated alleles identified in SNP-by-SNP association analyses into an aggregate class. LD calculations were performed using the genetics module of the R statistical analysis software package (41,42).

Association analyses

SNP-by-SNP genotype–phenotype associations were tested using the regression models in the R statistical analysis package (41). Tests for overall gene-specific and cross-gene effects were performed under mixed models for repeated measures with SAS (SAS Institute Inc., Cary, NC, USA), treating genotype as independent variable and log-transformed thresholds as dependent variables. Similarly, haplotype-specific and cross-gene effects were performed treating haplotype-carrier status as an independent variable, and only haplotypes with frequencies >0.05 were included in these analyses.

Functional assays

The functional characteristics of individual receptor alleles were determined using heterologous expression and calcium imaging assays developed in the course of previous studies (22). Receptor variants were amplified from genotyped DNA samples and subcloned into the pcDNA5/FRT/TO expression vector (Invitrogen, Carlsbad, CA, USA), which was appended with an N-terminal plasma membrane-targeting sequence consisting of the amino acids 1–45 of the rat somatostatin type 3 receptor to ensure cell-surface localization which the C-terminal HSV tag was omitted. Additional constructs, composed of single- and double-point mutations introduced to target alleles, were generated using the QuickChange protocol (Stratagene, Inc., La Jolla, CA, USA) according to the manufacturers' recommendations. The correctness of all constructs was checked prior to functional analysis by sequencing.

Functional expression analyses were carried out in a HEK293-Flp-In T-REx cell line (Invitrogen) stably expressing human phospholipase-C-β2 (PLCβ2) under control of an inducible tetracycline promoter. Each construct was transiently co-transfected with PLCβ2 and the G protein subunits, α-gustducin, β-3 and γ-13 in equal amounts, to enable correct signaling. Empty pcDNA5/FRT vector was used as negative control. Twenty-four to 32 h post transfection and induction of PLCβ2 expression, calcium imaging was performed by exposing transfected cells to solutions of saccharin (5 mM), acesulfame K (5 mM) dissolved in C1 solution (130 mM NaCl, 5 mM KCl, 10 mM HEPES, 2 mM $CaCl_2$ and 1 mM glucose, pH 7.4), and recording responses with an automated fluorometric imaging plate reader (Molecular Devices, Inc., Sunnyvale, CA, USA). Following exposure, cell vitality was verified by applying 100 nM endogenous somatostatin receptor type 2 (Bachem AG, Bubendorf, Switzerland). Dose–response data were collected from a minimum of three independent experiments, which were performed at least in duplicate. Peak fluorescence responses after exposure were normalized to background fluorescence ($\Delta F/F = (F-F0)/F0$) and baseline noise was subtracted.

SUPPLEMENTARY MATERIAL

Supplementary Material is available at *HMG* online.

ACKNOWLEDGEMENTS

The authors thank Mrs Elke Chudoba, Mrs Ellen Schöley-Pohl, Mrs Renate Schröder and Mrs Stephanie Schultz

(all Nuthetal) for technical assistance and Ms Jenny Stehr (Nuthetal) and Dr Marcel Winnig (Milan) for help with the functional expression assay. The contributions of Ms Anika Engel (Nuthetal) and Ms Anna Sinnak (Nuthetal) to the sensory experiments are acknowledged.

Conflict of Interest statement. None declared.

FUNDING

The work was supported by a grant of the German Research Foundation (DFG) to W.M. (Me 1024/2-3).

REFERENCES

1. Sandell, M. and Breslin, P. (2006) Variability in a taste-receptor gene determines whether we taste toxins in food. *Curr. Biol.*, **16**, R792–R794.
2. Dinehart, M., Hayes, J., Bartoshuk, L., Lanier, S. and Duffy, V. (2006) Bitter taste markers explain variability in vegetable sweetness, bitterness, and intake. *Physiol. Behav.*, **87**, 304–313.
3. Drewnowski, A., Henderson, S. and Barratt-Fornell, A. (2001) Genetic taste markers and food preferences. *Drug Metab. Dispos.*, **29**, 535–538.
4. Duffy, V. (2004) Associations between oral sensation, dietary behaviors and risk of cardiovascular disease (CVD). *Appetite*, **43**, 5–9.
5. Fischer, R., Griffin, F. and Kaplan, A.R. (1963) Taste thresholds, cigarette smoking, and food dislikes. *Med. Exp. Int. J. Exp. Med.*, **210**, 151–167.
6. Tepper, B.J. (1998) 6-n-Propylthiouracil: a genetic marker for taste, with implications for food preference and dietary habits. *Am. J. Hum. Genet.*, **63**, 1271–1276.
7. Duffy, V.B., Davidson, A.C., Kidd, J.R., Kidd, K.K., Speed, W.C., Pakstis, A.J., Reed, D.R., Snyder, D.J. and Bartoshuk, L.M. (2004) Bitter receptor gene (TAS2R38), 6-n-propylthiouracil (PROP) bitterness and alcohol intake. *Alcohol Clin. Exp. Res.*, **28**, 1629–1637.
8. Cannon, D.S., Baker, T.B., Piper, M.E., Scholand, M.B., Lawrence, D.L., Drayna, D.T., McMahon, W.M., Villegas, G.M., Caton, T.C., Coon, H. *et al.* (2005) Associations between phenylthiocarbamide gene polymorphisms and cigarette smoking. *Nicotine Tob. Res.*, **7**, 853–858.
9. Enoch, M.A., Harris, C.R. and Goldman, D. (2001) Does a reduced sensitivity to bitter taste increase the risk of becoming nicotine addicted?. *Addict. Behav.*, **26**, 399–404.
10. Goldstein, G.L., Daun, H. and Tepper, B.J. (2005) Adiposity in middle-aged women is associated with genetic taste blindness to 6-n-propylthiouracil. *Obes. Res.*, **13**, 1017–1023.
11. Basson, M.D., Bartoshuk, L.M., Dichello, S.Z., Panzini, L., Weiffenbach, J.M. and Duffy, V.B. (2005) Association between 6-n-propylthiouracil (PROP) bitterness and colonic neoplasms. *Dig. Dis. Sci.*, **50**, 483–489.
12. Adler, E., Hoon, M.A., Mueller, K.L., Chandrashekar, J., Ryba, N.J. and Zuker, C.S. (2000) A novel family of mammalian taste receptors. *Cell*, **100**, 693–702.
13. Chandrashekar, J., Mueller, K.L., Hoon, M.A., Adler, E., Feng, L., Guo, W., Zuker, C.S. and Ryba, N.J. (2000) T2Rs function as bitter taste receptors. *Cell*, **100**, 703–711.
14. Bufe, B., Hofmann, T., Krautwurst, D., Raguse, J.D. and Meyerhof, W. (2002) The human TAS2R16 receptor mediates bitter taste in response to beta-glucopyranosides. *Nat. Genet.*, **32**, 397–401.
15. Roper, S. (2007) Signal transduction and information processing in mammalian taste buds. *Pflugers Arch.*, **454**, 759–776.
16. Tizzano, M., Gulbransen, B.D., Vandenbeuch, A., Clapp, T.R., Herman, J.P., Sibhatu, H.M., Churchill, M.E., Silver, W.L., Kinnamon, S.C. and Finger, T.E. (2010) Nasal chemosensory cells use bitter taste signaling to detect irritants and bacterial signals. *Proc. Natl Acad. Sci. USA*, **107**, 3210–3215.
17. Shah, A.S., Ben-Shahar, Y., Moninger, T.O., Kline, J.N. and Welsh, M.J. (2009) Motile cilia of human airway epithelia are chemosensory. *Science*, **325**, 1131–1134.
18. Rozengurt, E. and Sternini, C. (2007) Taste receptor signaling in the mammalian gut. *Curr. Opin. Pharmacol.*, **7**, 557–562.
19. Drayna, D. (2005) Human taste genetics. *Annu. Rev. Genomics Hum. Genet.*, **6**, 217–235.
20. Drayna, D., Coon, H., Kim, U.K., Elsner, T., Cromer, K., Otterud, B., Baird, L., Peiffer, A.P. and Leppert, M. (2003) Genetic analysis of a complex trait in the Utah Genetic Reference Project: a major locus for PTC taste ability on chromosome 7q and a secondary locus on chromosome 16p. *Hum. Genet.*, **112**, 567–572.
21. Kim, U.K., Jorgenson, E., Coon, H., Leppert, M., Risch, N. and Drayna, D. (2003) Positional cloning of the human quantitative trait locus underlying taste sensitivity to phenylthiocarbamide. *Science*, **299**, 1221–1225.
22. Meyerhof, W., Batram, C., Kuhn, C., Brockhoff, A., Chudoba, E., Bufe, B., Appendino, G. and Behrens, M. (2010) The molecular receptive ranges of human TAS2R bitter taste receptors. *Chem. Senses*, **35**, 157–170.
23. Schiffman, S.S., Crofton, V.A. and Beeker, T.G. (1985) Sensory evaluation of soft drinks with various sweeteners. *Physiol. Behav.*, **34**, 369–377.
24. Horne, J., Lawless, H.T., Speirs, W. and Sposato, D. (2002) Bitter taste of saccharin and acesulfame-K. *Chem. Senses*, **27**, 31–38.
25. Schiffman, S.S. and Gatlin, C.A. (1993) Sweeteners: state of knowledge review. *Neurosci. Biobehav. Rev.*, **17**, 313–345.
26. Helgren, F.J., Lynch, M.J. and Kirchmeyer, F.J. (1955) A taste panel study of the saccharin off-taste. *J. Am. Pharm. (Baltim.)*, **44**, 353–355.
27. Pronin, A.N., Tang, H., Connor, J. and Keung, W. (2004) Identification of ligands for two human bitter T2R receptors. *Chem. Senses*, **29**, 583–593.
28. Kuhn, C., Bufe, B., Winnig, M., Hofmann, T., Frank, O., Behrens, M., Lewtschenko, T., Slack, J.P., Ward, C.D. and Meyerhof, W. (2004) Bitter taste receptors for saccharin and acesulfame K. *J. Neurosci.*, **24**, 10260–10265.
29. Pronin, A., Xu, H., Tang, H., Zhang, L., Li, Q. and Li, X. (2007) Specific alleles of bitter receptor genes influence human sensitivity to the bitterness of aloin and saccharin. *Curr. Biol.*, **17**, 1403–1408.
30. Shi, P., Zhang, J., Yang, H. and Zhang, Y.P. (2003) Adaptive diversification of bitter taste receptor genes in Mammalian evolution. *Mol. Biol. Evol.*, **20**, 805–814.
31. Blakeslee, A.F. and Salmon, M.R. (1935) Genetics of sensory thresholds: individual taste reactions for different substances. *Proc. Natl Acad. Sci. USA*, **21**, 84–90.
32. Nekrutenko, A., Makova, K.D. and Li, W.H. (2002) The K(A)/K(S) ratio test for assessing the protein-coding potential of genomic regions: an empirical and simulation study. *Genome Res.*, **12**, 198–202.
33. Kim, U., Wooding, S., Ricci, D., Jorde, L.B. and Drayna, D. (2005) Worldwide haplotype diversity and coding sequence variation at human bitter taste receptor loci. *Hum. Mutat.*, **26**, 199–204.
34. Meyerhof, W., Behrens, M., Brockhoff, A., Bufe, B. and Kuhn, C. (2005) Human bitter taste perception. *Chem. Senses*, **30**(Suppl. 1), i14–i15.
35. Fushan, A.A., Simons, C.T., Slack, J.P. and Drayna, D. (2010) Association between common variation in genes encoding sweet taste signaling components and human sucrose perception. *Chem. Senses*, **35**, 579–592.
36. Reed, D.R., Zhu, G., Breslin, P.A., Duke, F.F., Henders, A.K., Campbell, M.J., Montgomery, G.W., Medland, S.E., Martin, N.G. and Wright, M.J. (2010) The perception of quinine taste intensity is associated with common genetic variants in a bitter receptor cluster on chromosome 12. *Hum. Mol. Genet.*, **19**, 4278–4285.
37. Soranzo, N., Bufe, B., Sabeti, P.C., Wilson, J.F., Weale, M.E., Marguerie, R., Meyerhof, W. and Goldstein, D.B. (2005) Positive selection on a high-sensitivity allele of the human bitter-taste receptor TAS2R16. *Curr. Biol.*, **15**, 1257–1265.
38. Sudmant, P.H., Kitzman, J.O., Antonacci, F., Alkan, C., Malig, M., Tsalenko, A., Sampas, N., Bruhn, L., Shendure, J. *et al.* 1000 Genomes Project. (2010) Diversity of human copy number variation and multicopy genes. *Science*, **330**, 641–646.
39. Stephens, M., Smith, N.J. and Donnelly, P. (2001) A new statistical method for haplotype reconstruction from population data. *Am. J. Hum. Genet.*, **68**, 978–989.
40. Slatkin, M. (2008) Linkage disequilibrium—understanding the evolutionary past and mapping the medical future. *Nat. Rev. Genet.*, **9**, 477–485.
41. R Development Core Team. (2010) *R: A Language and Environment for Statistical Computing*. R Foundation for Statistical Computing, Vienna, Austria.
42. Warnes, G., Gorjanc, G., Leisch, F. and Man, M. (2008) *Package 'genetics'*. Rochester, NY.